JVSTB Journal of Vacuum Science & Technology B

Imaging of soft structures: Dependence of contrast in atomic force microscopy images on the force applied by the tip

O. Teschke, G. Ceotto, and E. F. de Souza

Citation: Journal of Vacuum Science & Technology B **18**, 1144 (2000); doi: 10.1116/1.591350

View online: http://dx.doi.org/10.1116/1.591350

View Table of Contents: http://scitation.aip.org/content/avs/journal/jvstb/18/3?ver=pdfcov

Published by the AVS: Science & Technology of Materials, Interfaces, and Processing

Imaging of soft structures: Dependence of contrast in atomic force microscopy images on the force applied by the tip

O. Teschke[a)]
Nano-Structure Laboratory, IFGW/UNICAMP, 13081-970 Campinas, SP, Brazil

G. Ceotto
Departamento de Fisica, Universidade Federal de Vicosa, 36571-000 Vicosa, MG, Brazil

E. F. de Souza
Instituto de Ciencias Biologicas e Quimica, Pontificia Universidade Catolica de Campinas, 13020-904 Campinas, SP, Brazil

(Received 13 September 1999; accepted 10 March 2000)

Forces acting on atomic force microscope tips during scanning of films of ionic surfactant molecules adsorbed from aqueous solutions onto hydrophilic substrates are measured. Near critical micellar concentration images of mica substrates show aggregate regions at the interface. Force versus distance curves indicate that aggregates are the thickest adsorbed structures on the substrate. However, topographic images registered at low scanning speed (15 μm/s) show that these aggregates appear as holes, consequently observed as inverted in contrast images. In atomic force microscope imaging of soft structures such as surfactants or biological material, inverted images may be observed when the tip penetrates the scanned layers. This penetration can be adjusted by changing the force applied by the tip, which results in different images. In order to obtain the conventional atomic force microscope contrast in scanned images the applied force set point is determined by the analysis of the force versus distance curves. © *2000 American Vacuum Society*. [S0734-211X(00)11803-7]

I. INTRODUCTION

Properties of surfactant films are of great technological importance for the lubrication of a miniaturized mechanical device.[1] In addition, understanding the adsorption mechanism of surfactant molecules at the solid-liquid interface, is an important step toward modeling industrial processes which use surfactants on a large scale, such as detergents, water purification, oil recovery, and ore refinement by flotation.[2] An intermolecular interaction in bulk solution leads to a variety of self-assembled structures like micelles or liquid-crystalline structures which have been well studied.[3] At an interface, however, the normal self-assembly process is perturbed by competing surfactant-surface and solvent-surface interactions, which can, in principle, lead to novel structures called ''hemimicelles.''[4] Over the last few decades, the adsorption characteristics of a wide variety of surfactant-solvent-substrate systems have been investigated, traditionally by adsorption isotherm[5] and more recently by fluorescence decay[6] and neutron reflection.[7]

Imaging hard samples with atomic resolution requires a probe with atomic dimensions. The atomic force microscope (AFM) obtains topographical information from the short-range repulsion resulting from the overlap of electronic shells between the tip and sample.[8] However, the presence of long-range interactions such as the double layer electrostatic force[9–13] when scanning soft samples in liquid media leads to a very different imaging scenario. The purpose of this article is to report on forces acting on the tip when imaging soft samples, as surfactant layers, in liquid media and to determine their effects on the AFM image contrast. Images of soft layers have been previously reported.[14–17] Here the effect of the applied force on the AFM image contrast was investigated. Patches formed by solvent-surfactant-substrate systems at mica surfaces in 1×10^{-5}, 3×10^{-5}, and 5×10^{-5} M CTAB [cetyltrimethylammonium bromide, $C_{16}H_{33}(CH_3)_3N^+Br^-$ (CTAB), cmc = 0.9 mM] solutions were imaged and also characterized by force versus distance measurements.

II. EXPERIMENT

Adsorption and self-assembly of the cationic surfactant CTAB was investigated at the interface between an aqueous solution and a hydrophilic substrate, namely, the cleavage plane of mica. Surfactant adsorption was accomplished by introducing an aqueous solution of CTAB into the fluid cell and allowing the tip and freshly cleaved substrate to stand in this solution for 50 min before operation. CTAB (99% purity) was used as supplied, without further purification. CTAB aqueous solutions using Milli-Q Plus quality (resistivity $\sim$10 MΩ/cm) were introduced into the cell after freshly cleaved mica was mounted on the *xyz* translator of the AFM.

In this study all force curves and images were obtained in surfactant solution at room temperature ($\sim$25 °C) by a commercial AFM (Topometrix TMX2000). A sensor using a four-quadrant detector measures vertical as well as lateral forces. Unmodified silicon nitride (Si_3N_4) tips[18] (Microlever™ type B, Park) was used. A special cell was built in

a)Electronic mail: oteschke@ifi.unicamp.br

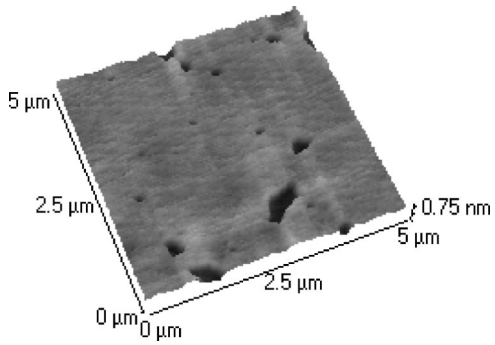

FIG. 1. AFM image of a CTAB adsorbed layer on mica in a 5×10^{-5} M CTAB solution. Lighter regions indicate higher structures.

order to perform observations in liquid media.[19,20] The cell was made of Teflon and the substrate (freshly cleaved mica) was fixed at its bottom. It was mounted in a *xyz* piezotranslator to position the sample in contact with a stationary tip. The laser beam enters and leaves the cell through a glass plate and thus does not cross the air-liquid interface, which is usually curved. We have obtained the best results in these measurements with very soft cantilevers, typically $\sim$0.02 N/m. Airborne contamination is minimized by preparing samples in a compact laminar flow cabinet and scanning samples in a clean air hood. The instrument was calibrated and the measured spring constant in air (0.023 nN/nm) was found to agree with that specified by the cantilever manufacturer.

The large range of the measured values of the force acting on the tip during the tip approach to the surface (force versus distance curves) published in the literature may be associated with the different tip fabrication procedures, resulting in various tip shapes, distinct radii of curvature of the tip end and distinct pyramidal cone angles. The tip composition (Si, Si_4N, or diamond covered tip, etc.) may also be a determinant factor in the force measured values as well as cantilever spring constant values starting from 0.01 up to 50 N/m.

When the mica basal plane is placed in pure water, the mechanism for the formation of the double layer is assumed to be the dissolution of K^+ ions as well as ion exchange of K^+ by H^+ or H_3O^+ ions. When CTAB is added to water K^+ is also substituted by $C_{16}H_{33}(CH_3)_3N^+$ ions. The ζ (zeta) potential at the macroscopic mica surface-water interface was measured using the plane-interface technique in the presence of 10^{-3} M KCl, and was found to be $\sim$125 mV within the *p*H range from 5 to 6.[21]

III. RESULTS AND DISCUSSION

Figure 1 shows an image taken at a CTAB concentration of about 5×10^{-5} M. For this concentration a light region and a few CTAB patches (dark regions) are observed, as previously reported by Neivandt *et al.*[22] The standard AFM contrast in images show high structures as light regions and low structures as dark, consequently a high structure with a few holes covers the observed area. An apparent height difference between the two layers (dark and light regions) of

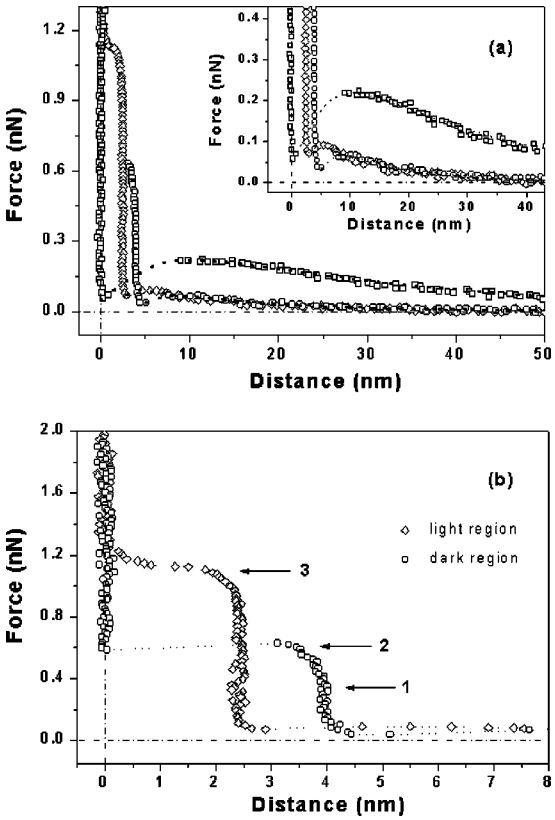

FIG. 2. (a) Force vs absolute distance curves for water (□), dark region (patches, ○), and light region (◇). Dashed lines are drawn to guide the eye. Inset: Same curve showing the details of the diffuse double layer. (b) Same force vs distance curves displayed in a region close (<8 nm) to the mica surface: dark region (curve ○) and light region (curve ◇).

0.5 nm was measured for a scanning speed of 15 μm/s. In order to determine the film thickness of each layer, force versus distance curves at the patches and at light regions were measured. In force versus distance curves,[23] the vertical axis represents the force acting between the tip and sample surface. Its value is obtained by multiplying the deflection of the cantilever with its spring constant. The horizontal axis (x) represents the distance the sample is moved perpendicular to the surface by the *xyz* translator. In this curve, repulsion acts between the tip and sample. Hence, when the sample approaches the tip, the cantilever bends upwards. At a certain point the tip is attracted to the surface. Finally, moving the sample still further causes a deflection of the cantilever by the same amount the sample is moved. A typical approaching force curve collected on a mica surface in CTAB solutions is a plot of the change in cantilever deflection (ΔY) versus sample displacement (ΔX). On a hard and nondeformable surface, ΔY is proportional to ΔX while the tip and the sample are in contact. Rather than using the sample position (X), it is more useful to use an absolute distance (D) that is the separation between the tip and the sample surface. The correction to produce a force versus distance curve uses the relationship $D=\Delta X-\Delta Y$.[24] Figure 2(a) shows the force versus absolute distances for the light area (curve ◇), the patch region (dark region, curve ○) and water (curve □).

Analysis of Fig. 2(a) shows that, at distances far away from the surfactant layer there is a force field that decays exponentially with distance with a Debye length (L_D)$\sim$27 nm, similar to the one obtained for bare mica in water (L_D $\sim$55 nm), curve □, in agreement with the value measured by Kékicheff *et al.*[25] The force intensity is decreased approximately by a factor of 3 compared to the value measured in water. This indicates the presence of an electric field generated by surface electric charges (mica), partially neutralized by surfactant adsorbed layer charges with the head groups in contact with the mica surface and exposed to the aqueous phase.

The strong repulsive forces at regions close to the substrate interface [$<$5 nm, Fig. 2(b)], in both curves (○ patches and ◇ light region forming the background structure), are associated with the adsorbed surfactant layer.[14,22] At $\sim$2.5 nm from the surface in the force curve (light area, curve ◇) there is a rapid change in force with a small change in tip/surface separation. One would imagine that the first step in this process might occur by rearrangement of the surfactant molecules at the tip/surface interaction region. After this initial step, interdigitation occurs between molecules in the layer and a monolayer is formed. The next component of the force is also repulsive and corresponds to squeezing of the monolayer patches resulting in the tilting of molecules. Finally, the surfactant layer is removed from the tip/substrate region.

A different surfactant structure is formed at the dark regions [Fig. 2(b), curve ○] as observed by the large repulsive deviation from the exponential component starting about 4.2 nm from contact and reaching a steep wall at approximately 4.0 nm.[14,22,26] A rapid change in force with almost no change in tip/substrate separation (at about 4.0 nm) followed by a second attractive regime (3.2 nm) is observed when the tip approaches the interface. This indicates that layer compression is followed by an attraction of the tip by the remaining material between the tip and substrate.

The distance measured from the contact point ($D = 0$) to the region of a sharp increase in the force value gives the surfactant layer thickness. The measured thicknesses of patches and of the light background region are $\sim$4.0 and 2.4 nm, respectively; dark areas are then thicker than light regions, and the film thickness difference measured from these curves is $\sim$1.6 nm. At sufficiently large applied force, the surfactant layer is squeezed from the space between the tip and the surface. This value is defined as the film rupture force and it is equal to 1.25 nN for the light region and 0.5 nN for the dark region. Previous results identify this rupture force with steric limitations imposed by the immobilization of CTAB and by the location of the CTAB binding site at the mica surface.[17]

The topographic image in Fig. 1 shows that the dark region forms shorter structures than the background, but the force versus distance curves show that the measured thickness of the dark region is 4.0 nm, and that of the light region 2.4 nm. The height variations of the different adsorbed structures measured during the scanning process and in the force versus distance curves acquisition stages are shown in Fig. 3.

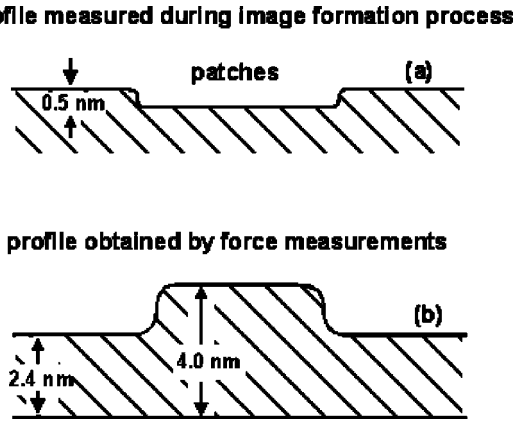

FIG. 3. Schematic diagram of the different stages present during sample scanning and the force vs distance measurements depicted by the relative height of the adsorbed structures.

In order to explain the inverted in contrast image shown in Fig. 1, conforming to the AFM practice that high structures are light and low structures are dark, the adsorbed patterns on the mica surface in different surfactant solution concentrations were observed. For mica immersed in 10^{-4}, 10^{-3}, and 10^{-2} M CTAB solutions, the surface is totally covered by patches. Layer rupture takes place 3.2 nm from the substrate. In these concentrations this width corresponds to the CTAB bilayer thickness.[14,25,27,28]

The velocity dependence effect on the measured thicknesses of the surfactant structures was then investigated. Figure 4 shows, for 5×10^{-5} M CTAB solutions, the force versus distance curves for various approach velocities for both structures. Each curve presented was registered using at least five different mica substrates and three different tips with various approach velocities averaged using measurements at different points on the sample. The step shown in the force versus distance curves is presented in all curves and all curves show the same thicknesses but the signal to noise ratio is variable. Therefore only the best signal noise ratio curves are presented here. The identical shape of the force

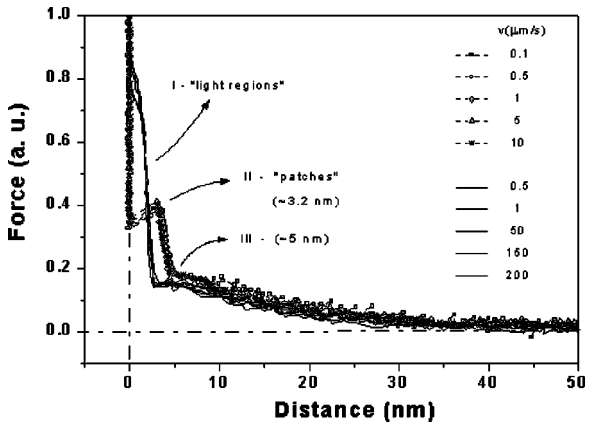

FIG. 4. Force vs absolute distance curves for water for different approach velocities.

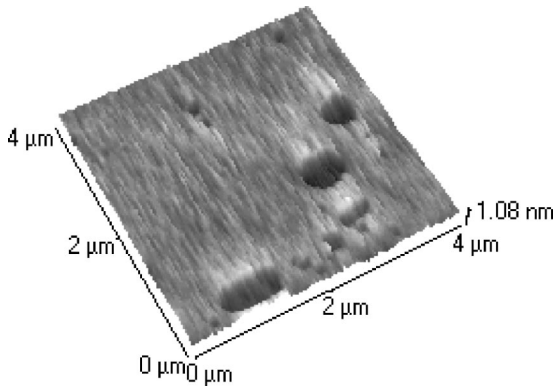

FIG. 5. AFM image of a CTAB adsorbed layer on mica in a 3×10^{-5} M CTAB solution; lighter regions indicate higher structures.

versus distance curves for both regions for various approach velocities indicates that there is no velocity dependence effect on the measured thicknesses of the surfactant at the structures. Additional images obtained at 3×10^{-5} and 1×10^{-5} M CTAB concentrations are shown in Figs. 5 and 6. For a 3×10^{-5} M CTAB concentration (see Fig. 5) the results are similar to those previously shown in Figs. 1–4 for 5×10^{-5} M CTAB. Figure 6(a) shows the pattern obtained in a 10^{-5} M CTAB aqueous solution. The profile of the image formed is shown in Fig. 6(b) and the corresponding force versus distance curve is shown in Fig. 6(c). The force versus distance curve obtained at the light regions shows that this structure has a 4.0 nm measured thickness relative to the mica substrate, consequently there is no inversion in contrast. A conventional AFM image is obtained in this case because there is no detectable penetration ($\sim$0.1 nm) through the hard substrate surface. The vertical profile measured using the scanned images, shown in Fig. 6(b), indicates that the light region (patches) has an height of $\sim$1.2 nm. The difference in height between the two measurements [shown in Figs. 6(b) and 6(c)] is associated with the tip penetration through the surfactant layer ($\sim$2 nm) during scanning. For a 1×10^{-5} M only bilayers are observed and the image has conventional image contrast since the background is a hard surface. Inverted in contrast images are only obtained when we scan various soft structures with differentiated tip penetration through each layer. We also observe that the area of the covered regions present at the mica surfaces decreases with decreasing CTAB concentrations.

The effect of the scanning speed on the image contrast was then investigated. An extra force associated with the scanning movement acts on the tip. A simple analogy for the observed phenomena is water skiing. In water skiing, the ski has to move faster than the water surface can rearrange. Consequently, the variable dynamic normal forces associated with the tip skiing at various scan speeds prevent the tip from penetrating through the layer. When comparing the measured height difference in Fig. 1, for dark and light regions, it is possible to determine, for each scanning speed, the value of the vertical force associated with the skiing of the tip. Since the measured height difference between the dark and the

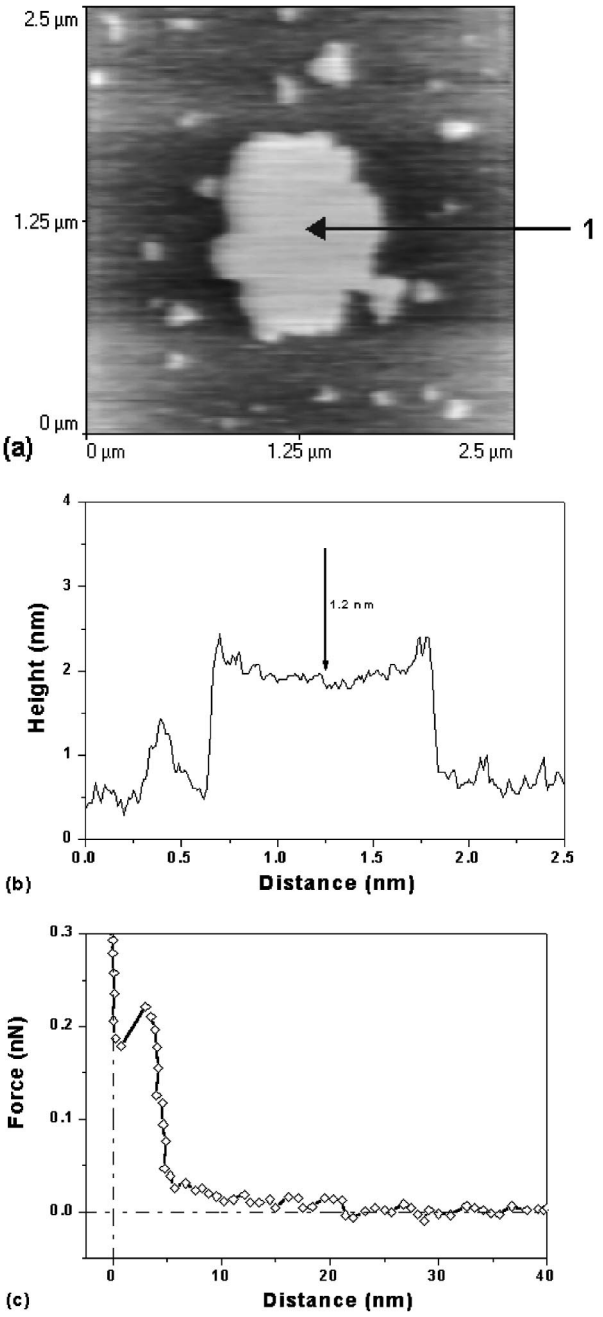

FIG. 6. (a) AFM image of a CTAB adsorbed layer on mica in a 1×10^{-5} M CTAB solution; lighter regions indicate higher structures. (b) Profile measured during the image formation process is indicated by the arrow in (a). (c) Force vs distance curve measured for points inside the light region indicated by the arrow in (a).

light region images in Fig. 1 is 0.5 nm, it is possible to determine the force component resulting from the tip skiing by determining the amplitude in the force versus distance curves that correspond to a height difference of 0.5 nm. The tip effective force is indicated by 2 in Fig. 2(b) which corresponds to a normal component of the skiing force of 2.0 nN (force set point 2.56 nN).

The effect of the tip's scanning speed on the image is observed in Figs. 7(a)–7(c) which display the pattern obtained for a force set point of 2.56 nN and the following

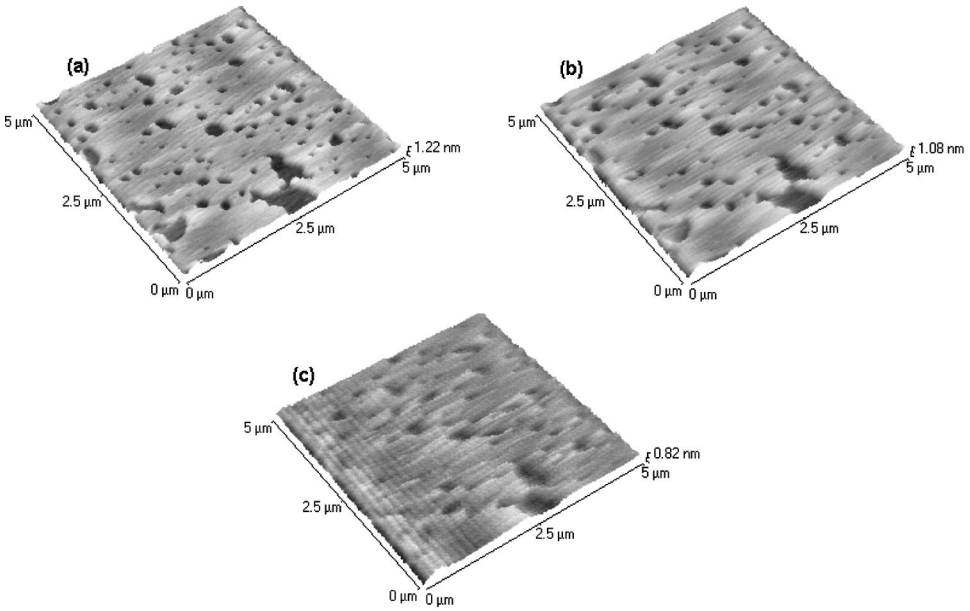

FIG. 7. AFM images of the solution/surfactant/mica interface for 2.56 nN applied force showing the tip scanning speed effect. (a) 15, (b) 50, and (c) 100 μm/s.

scanning speeds: 15, 50, and 100 μm/s, respectively. From 15 μm/s up to 50 μm/s the curves show identical images. For scanning speed greater than 50 μm/s the shape of the patches is drastically modified at each scanning. Inverted in contrast images were obtained for all scanning speeds, consequently, for the range of tested scanning velocities, no effect on the image contrast was observed.

A sequence of experiments was then performed, where an area was scanned for a constant scanning speed but with different tip applied forces. The result is given in Fig. 8; Fig. 8(a) shows the image obtained by scanning a mica CTAB covered region with a contact force of 2.56 nN; Fig. 8(b) shows the same scanned region divided into three subsets, each scanned with a different applied force: 2.56 (top), 0.12 (middle), and 3.66 nN (bottom). Finally, Fig. 8(c) was registered immediately after the scanning shown in Fig. 8(b). This image was also obtained with a contact force of 2.56 nN. The spatial distribution of the adsorbed surfactant layer on mica is shown in all images; the dark areas correspond to the patch regions and they are distributed in the background

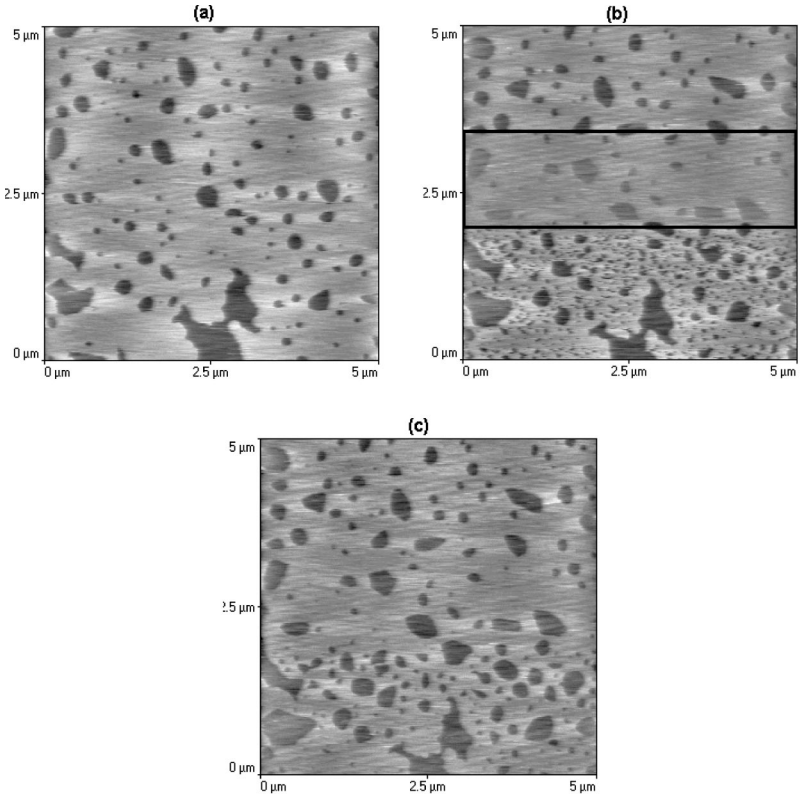

FIG. 8. AFM images of the solution surfactant/mica interface showing the tip force set point effect: (a) applied force of 2.56 nN, scanning speed 15 μm/s, (b) region scanned for different tip applied forces 2.56 (top), 0.12 (middle), and 3.66 nN (bottom); (c) image obtained after the scanned image shown in (b) for a tip applied force of 2.56 nN.

TABLE I. Total number of dark spots and the area of the dark region measured using the IMAGE PROPLUS 4.0 program.

Figure	Total count	Total area (arb units)
6(a)	168	17 616
6(b)	200	15 491
6(c)	146	15 844

of a light region. Inverted in contrast images are obtained for all measured applied forces. The effect of a variable applied force is quantified by measuring the height difference between patches and the light region for the three applied forces: ~ 0.5, ~ 0.3, and ~ 0.7 nN, respectively. The penetration of the tip through the light region and patches and consequently the AFM image contrast depends, then, on the applied force set point value.

The image shown in the bottom part of Fig. 8(b) presents a large number of small dark regions (patches) which were not present in the first scanned image. Since this image was obtained for the largest tip penetration through the surfactant layer it would be reasonable to assume that the removal of molecules from the light region will result in the formation of new small patches of surfactant molecules. Finally, in Fig. 8(c) we observe that after successive scans small patches tend to regroup, forming regions of larger patches.

Another point that deserves attention is that visual evaluation of the images [Figs. 8(a)–8(c)] shows that the total ''dark'' coverage seems to increase after large force scans. However, since free CTAB is present in solution and equilibrium should be achieved, the morphology might be altered by the tip scan, but not the coverage of each type. In order to clarify this point the area of the dark region in Figs. 8(a)–8(c) was measured. Initially the number of spots was counted and then the area of each spot determined using the Image Pro Plus 4.0 program, the results are shown in Table I. We observes that due to the scanning action the number of spots increases substantially in Fig. 8(b) and then decreases in Fig. 8(c). But the areas in Figs. 8(a)–8(c) are practically invariant (within 10%). In fact there is a decrease in the area of the dark regions after scan action which is the opposite result to the one obtained by visual evaluation of the images. The scan then modified the dark area by $\sim 10\%$ in a scanned area of $5 \times 5\ \mu m^2$ which corresponds to $\sim 10^{-7}$ of the total area of the sample ($1\ cm^2$).

Dark areas were then observed. The determining role played by the applied force set point in the image contrast is established when we change the applied force from 0.012 [Fig. 9(a)] to 2.56 nN [Fig. 9(b)]; a change in contrast occurred when the tip force was increased.

Considerable forces between the tip and sample are a requirement for AFM imaging. For hard samples, like mineral surfaces, these forces do not, generally, lead to any sample penetration. However, for organic films the minimum forces, which are barely enough to allow stable imaging, result in different tip penetration in each structure shown in Fig. 1 by the dark and light regions. In order to obtain conventional AFM contrast in the scanned samples, an analysis of the force versus distance curves is a requirement: let us observe Fig. 2(b) and consider the following simple scenario where we have an almost null vertical component due to the tip skiing. At the light region (curve $\diamondsuit$), by setting the contact force at 0.6 nN the tip is contacting the top of the surfactant layer. When the tip reaches the dark region the repulsive force is smaller than at the light region. Consequently, the tip gets closer to the substrate. A scanning profile that shows a smaller tip to substrate separation at the patch region than at the substrate is then registered, forming an inverted in contrast image. If the applied tip force varies from ~ 0.6 up to ~ 1.2 nN the same contrast image is obtained.

The total force on a tip when scanning is the sum of the vertical force component associated with tip skiing and the applied force. The true image profile of the surfactant structure would be obtained if the sum of forces on the tip (the sum of the applied force set value and the normal component force associated with the tip skiing) corresponds to the value indicated by 1 in Fig. 2(b) up to a total force of 0.5 nN. From these curves the patch height measured value is ~ 4.0 nm and the light region height is ~ 2.4 nm, as indicated by curves $\diamondsuit$ and $\bigcirc$.

Inverted in contract images may then formed when the tip scans soft layers where there is a differentiated tip penetration through each layer. However the observation by AFM of

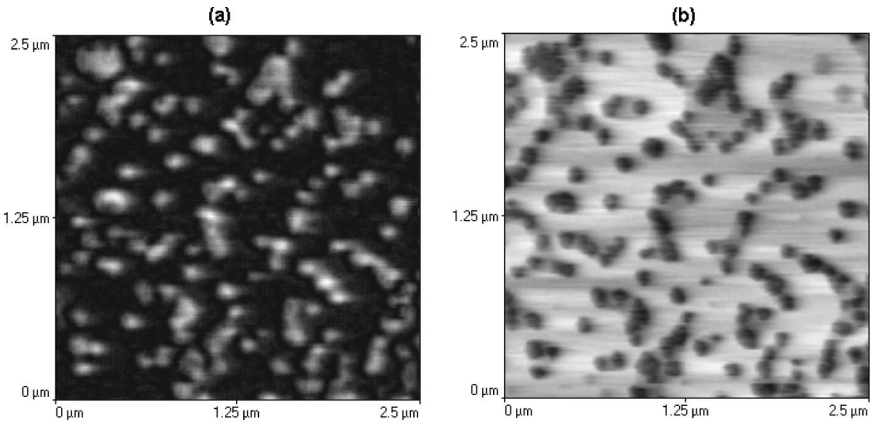

FIG. 9. AFM images of the solution/surfactant/mica interface scanned at different applied tip forces showing a change in image contrast: (a) 2.56 and (b) 0.012 nN.

only one soft structure adsorbed on a hard substrate as mica (Fig. 5) shows the standard contrast image.

The data obtained by force versus distance curves are then a requirement in order to measure the true layer thicknesses and determine the tip applied force set value for registering the AFM standard contrast in imaging surfaces. Large values of the sum of forces on the tip will result in the removal of the adsorbed layer, as indicated by 3 in Fig. 2(b), medium forces result in inverted in contrast images as indicated by 2 in Fig. 2(b), and the conventional image contrast is obtained for small forces, as indicated by 1 in Fig. 2(b).

IV. CONCLUSION

We have investigated the adsorbate structure formed by an ionic surfactant (CTAB) on a hydrophilic surface (mica) in contact with aqueous surfactant solutions. Fluid membranes can be imaged stably with a variable apparent height difference between various soft layers depending on the tip applied contact force. By adjusting the applied force and the scanning velocity conventional contrast may be obtained in imaging soft adsorbed layers. If high scanning speeds are used, transport of surfactant molecules by the tip from the light regions forming new dark regions is observed. The tip force set point value, needed to obtain the true profile of the structures, is determined from the force versus distance curves which show the force component normal to the scanned plane. High applied tip forces when scanning soft material will result in removal of the adsorbed layer, medium forces result in inverted contrast images, and the true image contrast is only obtained for small applied forces.

ACKNOWLEDGMENTS

The authors thank J. R. Castro and L. O. Bonugli for technical assistance. This work was supported by CNPq Grant No. 523.268/95-5 and FAPESP Grant No. 98/14769-2.

[1]J. Radler, M. Radmacher, and H. E. Gaub, Langmuir **10**, 3111 (1994).
[2]A. W. Adamson, *Physical Chemistry of Surfaces*, 5th ed. (Wiley, New York, 1990), Chap. XIII.
[3]J. N. Israelachvili, *Intermolecular and Surface Forces*, 2nd ed. (Academic, London, 1992).
[4]A. M. Gaudin and D. W. Fuerstenau, Trans. AIME **202**, 958 (1955).
[5]J. J. Kipling, *Adsorption from Solution of Non-Electrolytes* (Academic, London, 1965).
[6]P. Chandar, P. Somasundaran, and N. J. Turro, J. Colloid Interface Sci. **31**, 117 (1987).
[7]D. C. McDermott, J. McCarney, R. K. Thomas, and A. R. Rennie, J. Colloid Interface Sci. **162**, 304 (1994).
[8]F. V. Giesseibl, Phys. Rev. B **45**, 13815 (1992).
[9]O. Teschke and E. F. de Souza, Appl. Phys. Lett. **74**, 1755 (1999).
[10]O. Teschke and E. F. de Souza, Rev. Sci. Instrum. **69**, 3588 (1998).
[11]I. Y. Sokolov, G. S. Henderson, F. J. Wicks, and G. A. Ozin, Appl. Phys. Lett. **70**, 844 (1997).
[12]S. Manne, J. P. Cleveland, H. E. Gaub, G. D. Stucky, and P. K. Hansma, Langmuir **10**, 4409 (1994).
[13]W. A. Ducker and T. J. Senden, Langmuir **8**, 1831 (1992).
[14]M. W. Rutland and J. L. Parker, Langmuir **10**, 1110 (1994).
[15]J. Radler, H. Strey, and E. Sackmann, Langmuir **11**, 4539 (1995).
[16]G. S. Blackman, C. M. Mate, and M. R. Philpott, Phys. Rev. Lett. **65**, 2270 (1990).
[17]V. Yaminsky, C. Jones, F. Yaminsky, and B. W. Ninham, Langmuir **12**, 3531 (1996).
[18]Thermomicroscopes, 1171 Borregas Avenue, Sunnyvale, CA 94089.
[19]O. Teschke, R. A. Douglas, and T. A. Prolla, Appl. Phys. Lett. **70**, 1977 (1997).
[20]R. M. Sassaki, R. A. Douglas, M. U. Kleinke, and O. Teschke, J. Vac. Sci. Technol. B **14**, 2432 (1996).
[21]R. J. Hunter, *Foundations of Colloid Science* (Oxford University Press, New York, 1997).
[22]D. J. Neivandt, M. L. Gee, M. L. Hair, and C. P. Tripp, J. Phys. Chem. B **102**, 5107 (1988).
[23]W. A. Ducker, T. J. Senden, and R. A. Pashley, Langmuir **8**, 1831 (1992).
[24]H. J. Butt, M. Jaschke, and W. A. Ducker, Bioelectrochem. Bioenerg. **38**, 191 (1995).
[25]P. Ḱekicheff, H. Christenson, and B. W. Ninham, Colloids Surface **40**, 31 (1989).
[26]S. Manne, J. P. Cleveland, H. E. Gaub, G. D. Stucky, and P. K. Hansma, Langmuir **10**, 4409 (1994).
[27]A. R. Campanelli and L. Scaramuzza, Acta Crystallogr., Sect. C: Cryst. Struct. Commun. **42**, 1380 (1986).
[28]G. Fragneto, R. K. Thomas, A. R. Rennie, and J. Penfold, Langmuir **12**, 6036 (1996).